

Design and Uncertainty Evaluation of a Strain Measurement System

K. Kalita*, N. Das, P. K. Boruah and U. Sarma

Department of Instrumentation and USIC, Gauhati University, Guwahati, Assam 781014, India

Received: 17 April 2015 / Accepted: 21 October 2015

© Metrology Society of India 2015

Abstract: Strain measurement is very important in various industrial applications as well as different disciplines of science and technology for direct and indirect observations of certain parameters. Designing signal conditioning circuit is always a challenging and important task for satisfactory and reliable performance of a sensor as well as the system. The design and implementation details of a signal conditioning circuit of resistive sensor (strain gauge) for strain measurement are presented in this paper. Also the important aspects in designing a signal conditioning circuit for resistive sensor are presented and a novel method for the measurement of strain is discussed. Quarter bridge configuration with AC voltage excitation is used for the measurement along with the necessary circuitry to get a suitable and measurable output DC voltage. The measurement system is calibrated using a cantilever of stainless steel and the details of calibration are presented in the paper. The uncertainty associated with the measurement system is evaluated.

Keywords: Measurement uncertainty; Strain; Measurement systems; Calibration

1. Introduction

Strain gauges experience a change of an electrical parameter, usually their resistance, when they are stretched or strained being indestructibly located on special elastic elements [1, 2]. Strain gauges present a significant measurement challenge to measure mechanical movements in micro level. Accurate measurement of small change in resistance is critical in case of strain gauge [3].

Bridge circuits are a time-honored way to make accurate measurements of resistance and some other electrical parameters [4]. Wheatstone bridge offers a good method for measuring small resistance changes accurately and allows a differential measurement that offers a higher common-mode noise rejection than in a single-element measurement [5]. Therefore, it is used for sensing most of the resistive type sensors that include the measurement of temperature, strain, pressure, fluid flow, and relative humidity etc. Today, Wheatstone bridge is a basic structure for measurement in various measuring systems [6].

Several endeavours have been practiced and still going on to improve the quality of measurement using wheatstone bridge for its very high potential in the field of precision measurement. Yonce et al. developed a system for

DC autonulling bridge for real time resistance measurement. The DC autonulling bridge builds upon the wheatstone bridge configuration to measure sensor resistance by maximizing noise rejection and dynamic range, and also allowing real time monitoring of transient resistance changes [5]. Sun et al. [7] developed a signal conditioning and a data acquisition system including hardware and software implementation which can effectively measure weak signal using wheatstone bridge. A modified wheatstone bridge for the high-value resistance measurement from 1 M Ω to 1 T Ω is developed by Oe et al. [8]. The uncertainties of high resistance bridges are explained in that study. Boujamaa et al. proposed a feedback conditioning architecture to improve the power supply noise rejection of a wheatstone bridge [9]. Putter [10] has presented a paper on on-chip RC measurement and calibration circuit using wheatstone bridge. A fully automated measurement system has been developed for calibrating 1 Ω resistance standards using a modified wheatstone bridge by Hitoshi et al. [11].

In general strain gauges are used in a bridge configuration with a voltage or current excitation source. A strain-gauge test facility was designed and constructed to study the output signals resulting from gauges operating normally under sinusoidally varying strain and in two common failure modes, namely, debonding and loose termination by Ellis and Smith [12]. The widely used strain gauge bridge

*Corresponding author, E-mail: kunjatalakalita@yahoo.co.in

circuit topologies are quarter bridge, half bridge and full bridge configurations [13]. Pal et al. has developed and implemented for calibrating strain amplifiers used in strain data acquisition systems. The traceability for the strain measurement in terms of voltage has been established [14]. The output voltage variation is proportional to the relative resistance variation of the wheatstone bridge. The sensitivity of the bridge depends on type of bridge configuration used. The stability of the excitation voltage or current directly affects the overall accuracy of the bridge output. The excitation source may be voltage (AC or DC) or current.

All the strain measuring circuits have some amount of uncertainty associated with them. Walendziuk [15] studied the measurement uncertainty analysis of the strain gauge based stabilographic platform. For uncertainty analysis there are two approaches.

1. The Type A evaluation of standard uncertainty is the method of evaluation by the statistical analysis of observations [16–19].
2. The Type B evaluation of standard uncertainty is the method of evaluation by other information about the measurement [17–20].

In this paper a strain gauge based measurement system is presented. Quarter bridge configuration is chosen for reducing the uncertainty as well as the cost. The paper presents the details of a signal conditioning circuit to get the final output voltage in the form of DC although the bridge is excited with an AC voltage. The associated uncertainty of the system is evaluated for both A and B type and presented in the paper.

2. Description of Signal Conditioning Circuit

The block diagram of the signal conditioning circuit is shown in Fig. 1. The resistive strain gauge (part no. CF350-2AA(11)C20) has a nominal resistance of 350Ω with gauge factor $2.13 \pm 1 \%$. A 1 kHz, 16.52 V (peak to peak) sinusoidal signal from the Agilent Generator (model

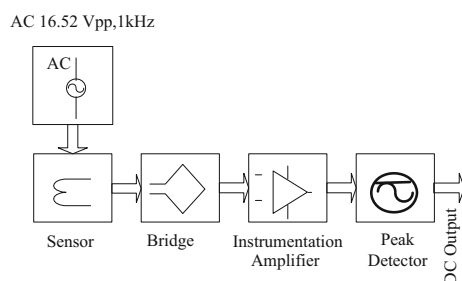


Fig. 1 Block diagram of the signal conditioning circuit of the resistive sensor

no. 33220A) is used to excite the bridge. The differential output of the bridge is amplified by the instrumentation amplifier (AD620) and the amplified AC output is converted to DC by using peak detector. AC excitation is more advantageous as it removes offset errors, average out $1/f$ noise, and eliminates effects due to parasitic thermocouples. Also the effects of electromagnetic interferences due to line frequency (50 Hz) are minimized.

3. Implementation

3.1. Bridge Design

Three resistors of $350 \Omega \pm 0.1 \%$ and temperature coefficient of $\pm 5 \text{ ppm}/^\circ\text{C}$ are used in the bridge. The strain gauge is connected to the fourth arm of the bridge (Fig. 2).

Use of 0.1% tolerance and temperature coefficient of $\pm 5 \text{ ppm}/^\circ\text{C}$ resistors ensures stability of bridge.

3.2. Sensitivity of the Bridge

The bridge output voltage, V_1 can be expressed as

$$V_1 = \frac{V_{in}}{4} \times \frac{\Delta R}{R} \quad (1)$$

where, V_1 is the output voltage, V_{in} the excitation voltage, ΔR the change in resistance of the sensor and R is the resistance of the sensor in the unstrained condition.

Gauge factor (GF) of a strain gauge is given by, [21]

$$GF = \frac{\Delta R/R}{\Delta L/L} = 2.13 \pm 1 \% \quad (2)$$

where, ΔL is the change in length of the specimen and L is original length of the specimen.

Using (1) and (2), the sensitivity is obtained as

$$\begin{aligned} \frac{V_1}{\Delta L/L} &= \frac{V_{in}}{4} \times GF \\ &= 8.80 \text{ V} \quad [\Delta L/L = \varepsilon = \text{strain}] \\ \frac{V_1}{\varepsilon} &= 8.80 \times 10^{-6} \text{ V}/\mu\text{strain} \end{aligned} \quad (3)$$

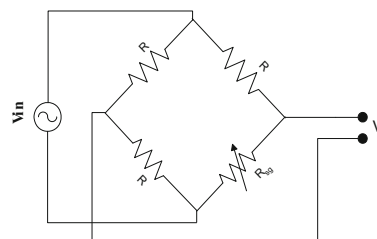


Fig. 2 Bridge circuit

3.3. Instrumentation Amplifier

AD620 is used to provide a gain of 495 and for removing any common mode signal coming out of the bridge. It is a high accuracy instrumentation amplifier that requires only one external resistor to set the gain in the range of 1–1000. The AD620, with its high accuracy of 40 ppm maximum nonlinearity, low offset voltage of 50 μ V maximum and offset drift of 0.6 μ V/ $^{\circ}$ C [22] (Fig. 3).

The gain equation is

$$G = \frac{49.4 \text{ k}\Omega}{R_g} + 1 \tag{4}$$

where, R_g is the gain setting resistor having value of 100 Ω . Therefore for our case, $G = 495$

3.4. Peak Detector

Peak detector circuit is shown in Fig. 4. The detected peak voltage charges the capacitor C3. The capacitor is discharged through R2 to store new value. Thus a DC voltage is obtained at the output. The DC output voltage V_{out} is given by

$$V_{out} = V_2/2 \tag{5}$$

where, V_2 is the peak to peak output of the instrumentation amplifier.

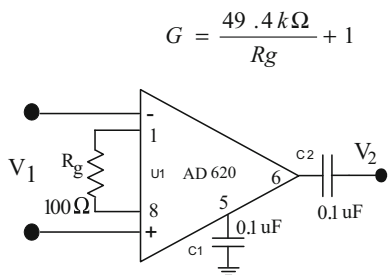


Fig. 3 Instrumentation amplifier circuit

3.5. Transfer Function of the System

Transfer function is derived as follows:

Voltage output (V_2) of the amplifier is

$$V_2 = \text{Gain} \times V_1 = \left(\frac{49.4 \text{ k}\Omega}{R_g} + 1 \right) \times \frac{V_{in}}{4} \times \frac{\Delta R}{R} \tag{6}$$

where, V_1 is the bridge output voltage.

Using (3) and (4), we get

$$\frac{V_2}{\epsilon} = \text{Gain} \times 8.8 \times 10^{-6} \text{ V}/\mu\text{strain}$$

$$\frac{V_2}{\epsilon} = \left(\frac{49.4 \text{ k}\Omega}{R_g} + 1 \right) \times 8.8 \times 10^{-6} \text{ V}/\mu\text{strain} \tag{7}$$

Since peak detector detects the peak of amplified output of the Instrumentation amplifier the transfer function becomes

$$\frac{V_{out}}{\epsilon} = \left(\frac{49.4 \text{ k}\Omega}{R_g} + 1 \right) \times 4.4 \times 10^{-6} \text{ V}/\mu\text{strain} \tag{8}$$

4. Calibration of the System

A rectangular beam of stainless steel is used to make a cantilever. The beam is fixed at one end and loaded at the other end using knife edge to remove shearing effect. The mass of the loads are measured by a balance (model no: AB54, make: Metler Toledo) prior to the experiment. Three strain gauges are attached to the surface of the beam with adhesive (cyanoacrylate) to measure tensile strain. Before attaching the strain gauges, the surface of the beam is cleaned and polished. The gauges are at X cm from the load. Strain gauge S_1 is at the principal axis (geometrically measured at the half of the width) of the beam which is used for calibration and S_2 and S_3 are at 3 mm from the principal axis used to study the effect of shearing strain (Fig. 5).

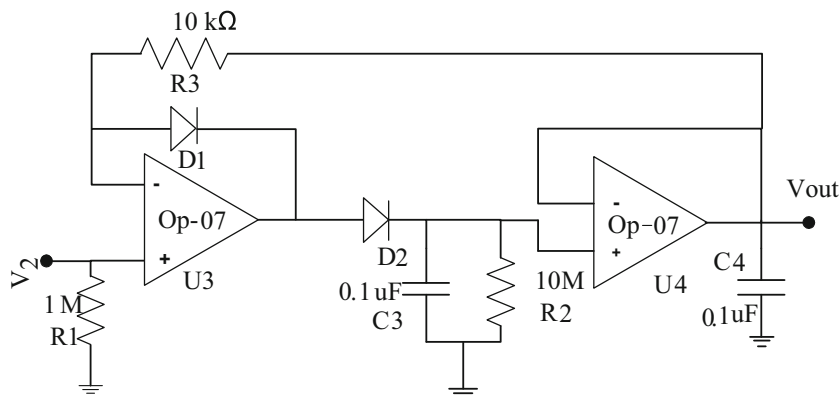


Fig. 4 Peak detector circuit

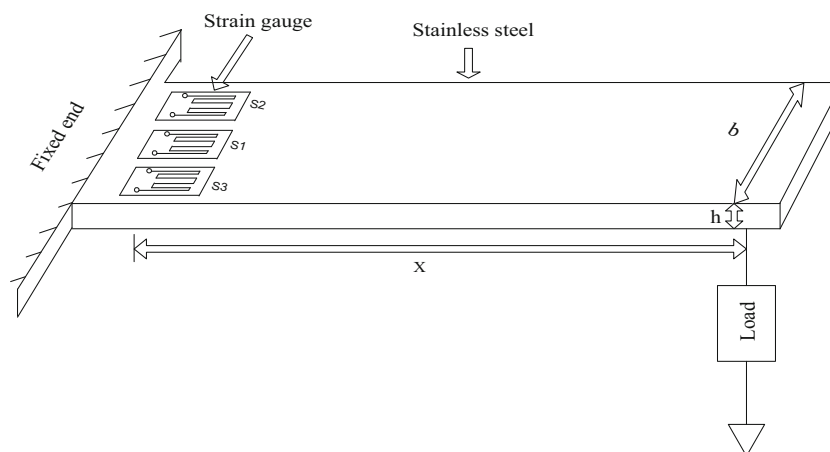


Fig. 5 System calibration setup

The bridge output of each of the strain gauges are measured independently using Agilent DMM (Model no: 34401A) and recorded.

The tensile strain (ε) for a cantilever is given by [23, 24]

$$\varepsilon = \frac{6 mgX}{bh^2E} \quad (9)$$

where, m is the mass of the load, g is the acceleration due to gravity (9.78049 m/s^2), X is the distance from the strain gauge to load (0.2 m), b is width of the cantilever beam (0.0184 m), h is thickness of the beam (0.00154 m), E is Young's modulus of the stainless steel ($180 \times 10^9 \text{ N m}^{-2}$).

The error in the measurement of tensile strain involves contribution from the measurements of the following factors m , X , b and h . The instrumental error in measuring m is $\partial m = 1 \times 10^{-7} \text{ kg}$,

$$\partial X = \partial b = \partial h = 1 \times 10^{-3} \text{ m.}$$

Hence, the total fractional error is calculated as

$$\begin{aligned} \frac{\delta(\varepsilon)}{\varepsilon} &= \sqrt{\frac{\delta_m^2}{m^2} + \delta_x^2 \left[\frac{1}{X^2} + \frac{1}{b^2} + \frac{1}{h^2} \right]} \\ &= 944.44 \times 10^{-3} \end{aligned}$$

The calculated strain and output voltages for different loads are shown in Table 1. Using Table 1 the output voltages for corresponding strain are plotted (shown in Fig. 6).

The data are fitted with a calibration curve as shown in Fig. 6.

The calibration curve is given as

$$y = 2.281x + 1286 \quad (10)$$

where, y represents the output voltage and x is the microstrain.

The slope of the fitted curve gives a measure of the sensitivity of the system in mV per microstrain. From this analysis, the error in output voltage is found to be 1.76 mV.

Table 1 Calculated strain and output voltages for different loads

Load m (gm)	Calculated μ strain using (9)	V_{out} (mV)
13.35	19.88	1332
20.27	30.19	1356
27.29	40.64	1381
55.00	81.91	1469
100.42	149.56	1625
149.42	222.53	1794
196.25	292.28	1954

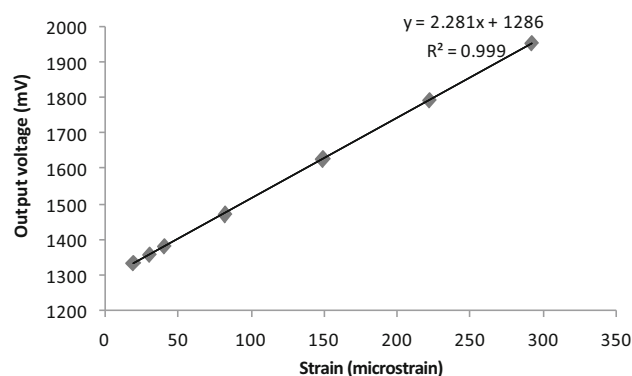


Fig. 6 Calibration curve

The deviation of the measured voltage from the expected value is shown in Fig. 7.

5. Effect of Sensor Misalignment

Misalignment of sensor may produce error in calibration. Due to sensor misalignment shearing strain may occur. To study the effect of shearing strain, the output voltages

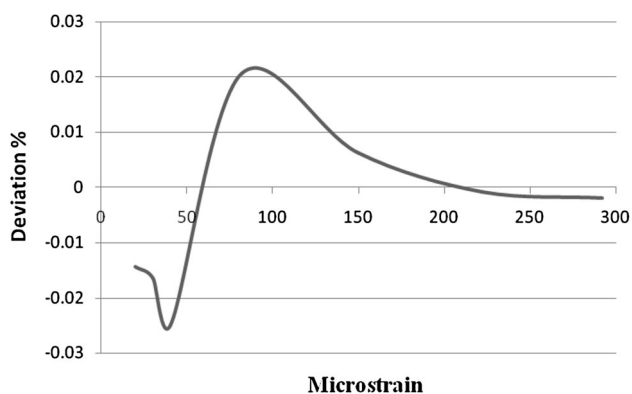


Fig. 7 Residual versus independent plot

Table 2 Sensitivity of the Sensors

Sensors	Sensitivity (mV/ μ strain)
S ₁	2.281
S ₂	2.221
S ₃	2.216

for the three sensors (shown in Fig. 5) are recorded and their corresponding sensitivities are observed using least square regression method. Table 2 shows the observations.

From the observation, it is found that the average change of sensitivity is 0.02 mV/ μ strain/mm due to misalignment of sensor from the principal axis. Therefore, the percentage change of sensitivity due to misalignment is 0.88 %/ μ strain/mm.

6. Uncertainty Evaluation of the System

6.1. Relative Uncertainty of the System

The uncertainty of the measurement system depends on various factors, e.g. the supply voltage of the bridge, tolerance of the fixed resistors and strain gauge. In order to calculate the value of measurement uncertainty the bridge output voltage (V_1) is fed to the instrumentation amplifier and the amplifier output voltage V_2 is applied to the peak detector circuit.

Now the DC output voltage is given by

$$V_{out} = \left(\frac{49.4 \text{ k}\Omega}{R_g} + 1 \right) \times \frac{V_{in}}{8} \times \frac{\Delta R}{R} \tag{11}$$

Excluding the constant terms (since they don't contribute uncertainty) relative uncertainty of the output, V_2 , is calculated as below.

$$\frac{u(V_2)}{V_2} = \sqrt{\left[\frac{u(R_g)}{R_g} \right]^2 + \left[\frac{u(V_{in})}{V_{in}} \right]^2 + \left[\frac{u(R_{sg})}{R_{sg}} \right]^2 + \left[\frac{u(R)}{R} \right]^2}$$

where, R_g is gain setting resistor with tolerance 1 %, V_{in} is excitation voltage, R_{sg} is strain gauge's resistance with tolerance 1 %, R is fixed resistor with tolerance 0.1 %.

$$\frac{u(V_2)}{V_2} = \sqrt{\left[\frac{1}{100} \right]^2 + \left[\frac{1}{8259} \right]^2 + \left[\frac{3.5}{350} \right]^2 + \left[\frac{.35}{350} \right]^2}$$

$$\frac{u(V_2)}{V_2} = 1.418 \times 10^{-2}$$

In the above calculation temperature coefficient of resistors (± 5 ppm/ $^{\circ}$ C) is ignored due to very small (1.43×10^{-6} %) contribution to uncertainty.

6.2. Type B Uncertainty Analysis

Type B uncertainties are tabulated in Table 3.

6.3. Type A Uncertainty Analysis

The Type A uncertainty analysis is done by the statistical data obtained from observations. The dominant sources of uncertainties are

- i) Bridge and
- ii) Signal Conditioning Circuit.

The estimated standard uncertainty (u) can be calculated as [16, 25, 26]

$$u = \frac{\sigma}{\sqrt{n}} \tag{12}$$

where, σ is standard deviation (SD), n is the number of measurements in a set.

The combined uncertainty (u_c) for two individual uncertainties u_1 and u_2 is calculated as [16]

Table 3 Standard type B uncertainty

Error sources	Error measure	Maximum possible error value (a)	Distribution type	Standard type B uncertainty
V_{in}	16.52 ± 1 mV	1 mV	Normal	1 mV
R_g	$100 \Omega \pm 1$ %	1 Ω	Rectangular	$\frac{1\Omega}{\sqrt{3}} = 0.58 \Omega$
R_{sg}	$350 \Omega \pm 1$ %	3.5 Ω	Rectangular	$\frac{3.5\Omega}{\sqrt{3}} = 2.02 \Omega$
R	$350 \Omega \pm 0.1$ %	0.35 Ω	Rectangular	$\frac{0.35\Omega}{\sqrt{3}} = 0.20 \Omega$

$$u_c = \sqrt{[u_1]^2 + [u_2]^2} \tag{13}$$

6.4. Uncertainty in Bridge

The bridge comprises of three resistors of nominal value 350 Ω with 0.1 % tolerance and temperature coefficient of ±5 ppm/°C and one strain gauge is connected to the fourth arm of the bridge. For unstrained condition, a dummy strain gauge is fixed in a FR4 PCB (insulating side) with adhesive (cyanoacrylate). The bridge is excited by a 1 kHz, 16.52 V (peak to peak) source.

To get the bridge output voltage, V_1 at unstrained condition (Fig. 2), 45 data are recorded by Agilent DMM (model no. 34401A). Figure 8 shows the variation of recorded ac voltage (Table 4).

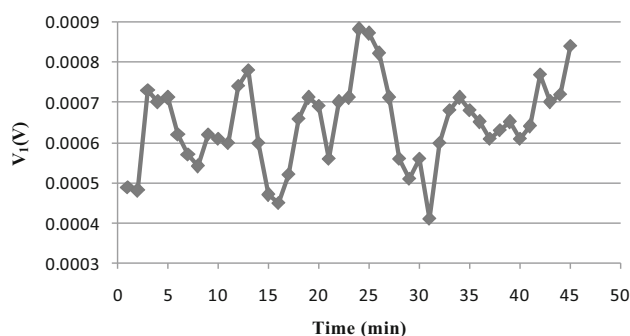


Fig. 8 Bridge output

Table 4 Type A uncertainty of the bridge

Bridge output	Average (mV)	SD (μV)	Standard uncertainty (u_1) (V)
V_1	646	109	1.63×10^{-5}

Table 5 Type A uncertainty of the signal conditioning circuit

Peak detector output	Average (V)	SD (mV)	Standard uncertainty (u_2) (V)
V_{out}	5	16.4	1.29×10^{-3}

6.5. Uncertainty in Signal Conditioning

To get the measurement uncertainty of the signal conditioning circuit, a 20 mV (peak to peak) signal from same function generator is applied to the input of the instrumentation amplifier. The recorded output voltage V_{out} of the system is shown in Fig. 9.

The average V_{out} is 5 V and the standard deviation of the signal conditioning circuit is 0.0164 V (Table 5).

6.6. Total Measurement Uncertainty of the System

Type A uncertainty in terms of μ strain is

$$\begin{aligned} \text{The combined uncertainty } (u_c) \text{ is} \\ &= \sqrt{[1.63 \times 10^{-5}]^2 + [1.29 \times 10^{-3}]^2} \\ &= 1.3 \times 10^{-3} \mu\text{strain} \end{aligned}$$

From the calibration Eq. (9), the sensitivity obtained is 2.281 mV/ μ strain.

Therefore, type A uncertainty in μ strain is estimated as

$$\frac{u_c}{2.281} = \frac{1.3}{2.281} = \pm 0.570 \mu\text{strain}$$

7. Uncertainty Comparison Between Full Bridge and Quarter Bridge

For full bridge, the relative uncertainty of the equivalent resistance of the bridge is calculated as

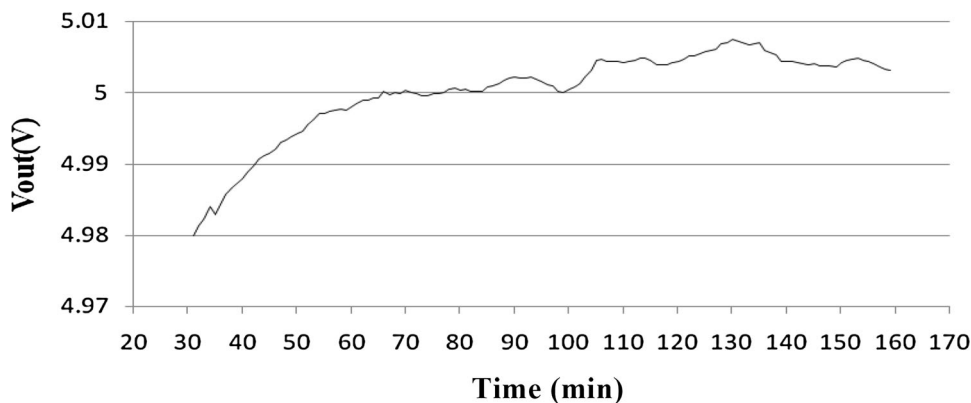


Fig. 9 Output voltage of the signal conditioning circuit

$$\begin{aligned}
&= \sqrt{\left[\frac{u(R_{sg})}{R_{sg}}\right]^2 + \left[\frac{u(R_{sg})}{R_{sg}}\right]^2 + \left[\frac{u(R_{sg})}{R_{sg}}\right]^2 + \left[\frac{u(R_{sg})}{R_{sg}}\right]^2} \\
&= \sqrt{\left[\frac{3.5}{350}\right]^2 + \left[\frac{3.5}{350}\right]^2 + \left[\frac{3.5}{350}\right]^2 + \left[\frac{3.5}{350}\right]^2} \\
&= 0.02
\end{aligned}$$

The relative uncertainty of the equivalent resistance of the quarter bridge is calculated as

$$\begin{aligned}
&= \sqrt{\left[\frac{u(R)}{R}\right]^2 + \left[\frac{u(R)}{R}\right]^2 + \left[\frac{u(R)}{R}\right]^2 + \left[\frac{u(R_{sg})}{R_{sg}}\right]^2} \\
&= \sqrt{\left[\frac{0.35}{350}\right]^2 + \left[\frac{0.35}{350}\right]^2 + \left[\frac{0.35}{350}\right]^2 + \left[\frac{3.5}{350}\right]^2} \\
&= 0.01
\end{aligned}$$

The relative uncertainty of the equivalent resistance is reduced to half in quarter bridge.

8. Conclusion

A strain measurement system is designed, developed and calibrated. The uncertainty associated with the system is evaluated. The sensitivity of the developed system obtained from the transfer function, (8), is 2.2 mV/ μ strain. The calibration equation, (10) gives the sensitivity of 2.1 mV/ μ strain i.e. the theoretical and the experimental results show a good agreement. The developed measurement system is capable of measuring strain in the range of microstrain with an uncertainty of $\pm 0.57 \mu$ strain.

The calibration is done using a reliable and convenient method which can be easily set up in a laboratory environment.

The bridge can be excited by DC, but AC excitation is more advantageous compared to DC such as keeping the excitation frequency greater than 50 Hz/60 Hz, the electromagnetic interference due to line frequency can easily be removed.

Since only one strain gauge is used in quarter bridge configuration, by using precision resistors (tolerance 0.1 %, temperature coefficient of ± 5 ppm/ $^{\circ}$ C) in the remaining three arms the resistance uncertainty of the bridge is 0.01 compared to full bridge configuration containing strain gauge of gauge factor 2.13 ± 1 % is 0.02.

Although temperature drift in the bridge is negligible due to use of precision resistor of low temperature coefficient (± 5 ppm/ $^{\circ}$ C), however, effect of temperature can be investigated.

Acknowledgments This study was supported in part by the Assam Science Technology and Environment Council (ASTEC), Assam

under Grant ASTEC/S&T/1614(2)/2012/3215. Dr. Kalyanee Boruah, Prof., Dept. of Physics, G.U., is also acknowledged.

References

- [1] R.B. Watson, Bonded electrical resistance strain gauge, Springer handbook of experimental solid mechanics, Springer. Available: <http://extras.springer.com/2008/978-0-387-26883-5/11510079/11510079-c-B-12/11510079-c-B-12.pdf>. Accessed 11 Mar 2014.
- [2] H. Kumar, M. Kaushik and A. Kumar, Development and characterization of a modified ring shaped force transducer, MAPAN-J. Metrol. Soc. India **30** (1) (2015) 37–47.
- [3] W. Kester, Sensor signal conditioning, Available: http://www.analog.com/library/analogdialogue/archives/39-05/web_ch4_final.pdf. Accessed 16 Feb 2015.
- [4] Tutorial 3426, Resistive bridge basics. Maxim Integrated Products, Inc. (2004). Available: <http://www.amdahl.com/doc/products/bsg/intra/infra/html> Accessed 20 Jan 2015.
- [5] D.J. Yonce, P.P. Bey and T.L. Fare, A DC autonulling bridge for real-time resistance measurement, IEEE Trans. Circuits Syst. I Fundam. Theory Appl. **47** (3) (2000) 273–278.
- [6] H.S. Yazdi and M. Rezaei, The wheatstone bridge-based analog adaptive filter with application in echo cancellation, Analog Integr Circuits Signal Process. **64** (2009) 191–198.
- [7] H. Sun, Y. Yu, R. Chen and Y. Ge, A signal conditioning and data acquisition system for micro/nano displacement sensor. International conference on robotics and biomimetics, Tianjin, China, December 2010 in Proceedings IEEE, 639–644 (2010).
- [8] T. Oe, J. Kinoshita and N. Kaneko, Voltage Injection type high ohm resistance bridge, Precis. Electromagn. Meas. Conf. IEEE (2012) 360–361.
- [9] B.E. Mehdi, F. Mailly, L. Latorre and P. Nouet, Improvement of power supply rejection ratio in wheatstone-bridge based piezoresistive MEMS, Analog Integr. Circuits Signal Process. **71** (2012) 1–9.
- [10] B.M. Putter, On-chip RC measurement and calibration circuit using wheatstone bridge, ISCAS IEEE (2008) 1496–1499.
- [11] H. Sasaki, H. Nishinaka and K. Shida, Automated measurement system for 1- Ω standard resistors using a modified wheatstone bridge, IEEE Trans. Instrum. Meas. **40** (2) (1991) 274–277.
- [12] B.L. Ellis and L.M. Smith, Modeling and experimental testing of strain gauges in operational and failure modes, IEEE Trans. Instrum. Meas. **58** (7) (2009) 2222–2227.
- [13] J. Bentley, Principles of measurement systems, 3rd edn. Pearson Education, New York, (2003).
- [14] B. Pal, A. Kumar, S. Madan, S. Ahmed and A.K. Govil, Establishment of traceability for strain measuring data acquisition system in terms of voltage, MAPAN-J. Metrol. Soc. India **25** (2) (2010) 125–128.
- [15] W. Walendziuk, Measurement uncertainty analysis of the strain gauge based stabilographic platform, Acta Mech. Autom. **8** (2014) 74–78.
- [16] S. Bell, A beginner's guide to humidity measurement. National Physical Laboratory, issue 2, NPL, (2011).
- [17] A.N. Johnson, C.J. Crowley and T.T. Yeh, Uncertainty analysis of NIST's 20 liter hydrocarbon liquid flow standard, MAPAN-J. Metrol. Soc. India **26** (2011) 187–202.
- [18] S. Yadav, B.V. Kumaraswamy, V.K. Gupta and A.K. Bandyopadhyay, Least squares best fit line method for the evaluation of measurement uncertainty with electromechanical transducers (emt) with electrical outputs (EO), MAPAN-J. Metrol. Soc. India **25** (2) (2010) 97–106.

- [19] M.S.B. Fernández, V.O. López and R.S. López, On the uncertainty evaluation for repeated measurements, *MAPAN-J. Metrol. Soc. India* **29** (1) (2014) 19–28.
- [20] U. Sarma and P.K. Boruah, Design and characterization of a temperature compensated relative humidity measurement system with on line data logging feature, *MAPAN-J. Metrol. Soc. India* **29** (2) (2014) 77–85.
- [21] Datasheet of CF350-2AA(11) C20. Available: www.nicsensorautomation.com. Accessed on 11 June 2014.
- [22] Datasheet of AD620. Available: www.analog.com. Accessed on 11 June 2014.
- [23] <http://media.paisley.ac.uk/~davison/labpage/gauges/gauges.html>. Accessed on 12 June 2014.
- [24] Y.A. Gilandeh and M. Khanramaki, Design, construction and calibration of a triaxial dynamometer for measuring forces and moments applied on tillage implements in field conditions, *MAPAN-J. Metrol. Soc. India* **28** (2) (2013) 119–127.
- [25] V.N. Ojha, Evaluation and expression of uncertainty of measurements, *MAPAN-J. Metrol. Soc. India* **13** (1998) 71–84.
- [26] D. Saikia, U. Sarma and P.K. Boruah, Development of an online heat Index measurement system for thermal comfort determination, *MAPAN-J. Metrol. Soc. India* **29** (2014) 67–72.